Applications in which standardized evaluation criteria will be beneficial particularly include assessments of the prophylactic or therapeutic efficacy of candidate vaccines or drugs that are on their way (14). In addition, the list can be helpful in determining differences in the virulence of virus isolates, effects of infectious dosage, comorbidities, age, or differences to other models including transgenic mice (4). In all scenarios, distinct study goals may justify different choices among the patterns proposed here. For example, perivascular lymphocytic cuffs may be relevant for the assessment of specific immune responses, as expected from vaccine trials, whereas aspects of regeneration and repair may be important age-related parameters. For any kind of comparative study, a bouquet of histologic quantification tools is already available that convert differences in each morphological parameter into statistically testable data, including scoring schemes (12), Cavalieri's principle (15), and computed digital image analyses (16).

We are only at the beginning of our understanding of COVID-19. The application of a structured, evidence-based catalog of relevant diagnostic criteria will certainly increase the value of information that can be obtained from animal models. ■

Author disclosures are available with the text of this letter at www.atsjournals.org.

Achim D. Gruber, D.V.M., Ph.D.*
Nikolaus Osterrieder, D.V.M.
Luca D. Bertzbach, D.V.M., Ph.D.
Daria Vladimirova, D.V.M.
Freie Universität Berlin
Berlin, Germany

Selina Greuel, M.D.
Jana Ihlow, M.D.
David Horst, M.D.
Charité–Universitätsmedizin Berlin
Berlin, Germany

Jakob Trimpert, D.V.M.‡
Kristina Dietert, D.V.M., Ph.D.‡
Freie Universität Berlin
Berlin, Germany

ORCID IDs: 0000-0002-4502-0393 (A.D.G.); 0000-0002-5313-2176 (N.O.); 0000-0002-0698-5395 (L.D.B.); 0000-0002-1562-4268 (D.V.); 0000-0001-5346-4499 (S.G.); 0000-0001-5484-1321 (J.I.); 0000-0003-4755-5743 (D.H.); 0000-0003-1616-0810 (J.T.); 0000-0002-5667-6750 (K.D.).

*Corresponding author (e-mail: achim.gruber@fu-berlin.de).
‡These authors contributed equally to this work.

References

1. Wichmann D, Sperhake JP, Lütgehetmann M, Steurer S, Edler C, Heinemann A, *et al*. Autopsy findings and venous thromboembolism in patients with COVID-19. *Ann Intern Med* [online ahead of print] 6 May 2020; DOI: 10.7326/M20-2003.
2. Hanley B, Lucas SB, Youd E, Swift B, Osborn M. Autopsy in suspected COVID-19 cases. *J Clin Pathol* 2020;73:239–242.
3. Ackermann M, Verleden SE, Kuehnel M, Haverich A, Welte T, Laenger F, *et al*. Pulmonary vascular endothelialitis, thrombosis, and angiogenesis in COVID-19. *New Engl J Med* 2020;383:120–128.
4. Le Bras A. Modeling SARS-CoV-2 infection in mice. *Lab Anim (NY)* 2020; 49:198.
5. Cleary SJ, Pitchford SC, Amison RT, Carrington R, Robaina Cabrera CL, Magnen M, *et al*. Animal models of mechanisms of SARS-CoV-2 infection and COVID-19 pathology. *Br J Pharmacol* [online ahead of print] 27 May 2020; DOI: 10.1111/bph.15143.
6. Rockx B, Kuiken T, Herfst S, Bestebroer T, Lamers MM, Oude Munnink BB, *et al*. Comparative pathogenesis of COVID-19, MERS, and SARS in a nonhuman primate model. *Science* 2020;368:1012–1015.
7. Yu P, Qi F, Xu Y, Li F, Liu P, Liu J, *et al*. Age-related rhesus macaque models of COVID-19. *Animal Model Exp Med* 2020;3:93–97.
8. Sia SF, Yan LM, Chin AWH, Fung K, Choy KT, Wong AYL, *et al*. Pathogenesis and transmission of Sars-CoV-2 in golden hamsters. *Nature* 2020;583:834–838.
9. Chan JF, Zhang AJ, Yuan S, Poon VK, Chan CC, Lee AC, *et al*. Simulation of the clinical and pathological manifestations of coronavirus disease 2019 (COVID-19) in golden syrian hamster model: implications for disease pathogenesis and transmissibility. *Clin Infect Dis* [online ahead of print] 26 Mar 2020; DOI: 10.1093/cid/ciaa325.
10. Imai M, Iwatsuki-Horimoto K, Hatta M, Loeber S, Halfmann PJ, Nakajima N, *et al*. Syrian hamsters as a small animal model for SARS-CoV-2 infection and countermeasure development. *Proc Natl Acad Sci USA* 2020;117:16587–16595.
11. Matute-Bello G, Downey G, Moore BB, Groshong SD, Matthay MA, Slutsky AS, *et al*.; Acute Lung Injury in Animals Study Group. An official American Thoracic Society workshop report: features and measurements of experimental acute lung injury in animals. *Am J Respir Cell Mol Biol* 2011;44:725–738.
12. Dietert K, Gutbier B, Wienhold SM, Reppe K, Jiang X, Yao L, *et al*. Spectrum of pathogen- and model-specific histopathologies in mouse models of acute pneumonia. *PLoS One* 2017;12:e0188251.
13. Osterrieder N, Bertzbach LD, Dietert K, Abdelgawad A, Vladimirova D, Kunec D, *et al*. Age-dependent progression of sars-cov-2 infection in syrian hamsters. *Viruses* 2020;12:779.
14. Kreye J, Reincke SM, Kornau HC, Sanchez-Sendin E, Corman VM, Liu H, *et al*. A SARS-CoV-2 neutralizing antibody protects from lung pathology in a COVID-19 hamster model. *Cell* [online ahead of print] 23 Sep 2020; DOI: 10.1016/j.cell.2020.09.049.
15. Dietert K, Reppe K, Mundhenk L, Witzenrath M, Gruber AD. mCLCA3 modulates IL-17 and CXCL-1 induction and leukocyte recruitment in murine Staphylococcus aureus pneumonia. *PLoS One* 2014;9:e102606.
16. Dietert K, Nouailles G, Gutbier B, Reppe K, Berger S, Jiang X, *et al*. Digital image analyses on whole-lung slides in mouse models of acute pneumonia. *Am J Respir Cell Mol Biol* 2018;58:440–448.

Effects of Asthma and Human Rhinovirus A16 on the Expression of SARS-CoV-2 Entry Factors in Human Airway Epithelium

To the Editor:

The factors that facilitate and impact transmission of the severe acute respiratory syndrome coronavirus 2 (SARS-CoV-2) are not well understood, particularly in children and young adults. It has been established that the S (Spike) protein of SARS-CoV-2 binds to ACE2 (angiotensin-converting enzyme 2) as the entry receptor and employs the serine protease TMPRSS2 for proteolytic separation of

Supported by U.S. National Institutes of Health Grants U19AI125378 (S.F.Z.), K24AI150991 (J.S.D.), R01HL089215, and K24AI130263 (T.S.H.).

Originally Published in Press as DOI: 10.1165/rcmb.2020-0394LE on September 18, 2020

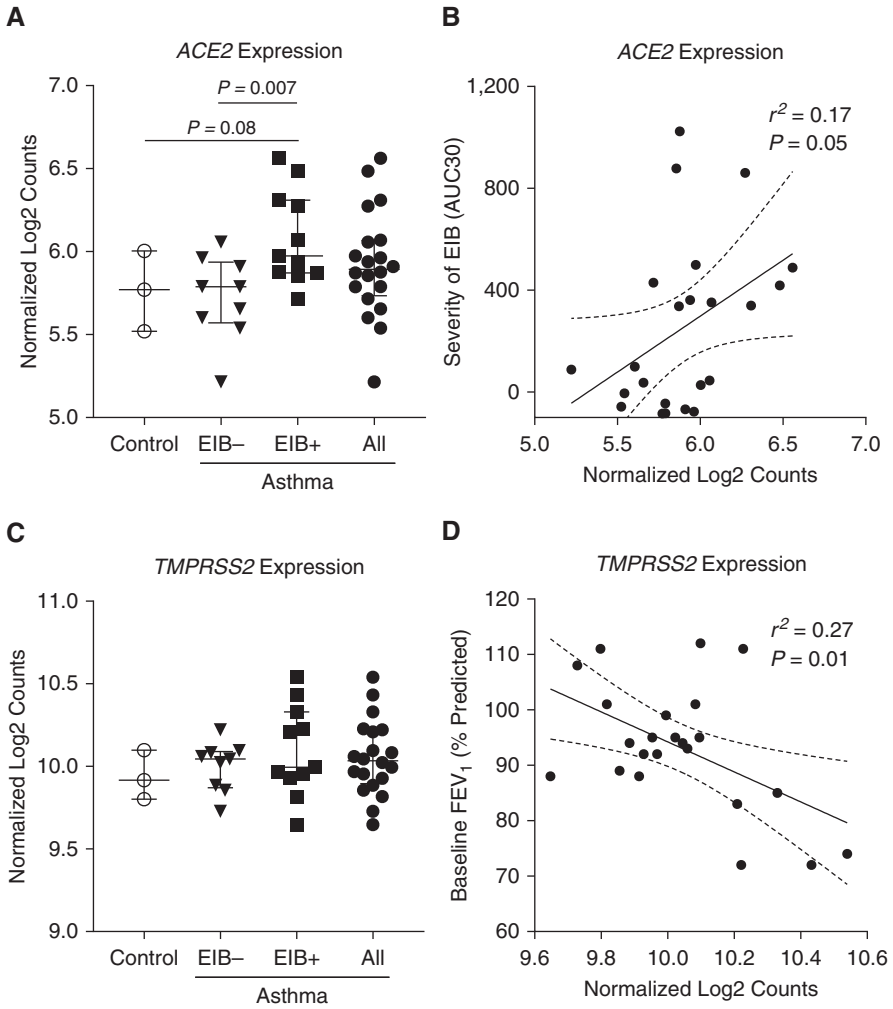

Figure 1. Epithelial brushings were obtained via bronchoscopy from the fourth- and fifth- generation airways from a cohort of individuals with and without asthma, and for those with asthma, with and without exercise-induced bronchoconstriction (EIB) (control, $n = 3$; EIB−, $n = 9$; EIB+, $n = 11$). (*A* and *C*) *ACE2* (angiotensin-converting enzyme 2) expression (*A*) and *TMPRSS2* expression (*C*) were quantified by normalized log2 counts. Median values with interquartile ranges are shown. *P* values represent the result of a one-way ANOVA. There was a trend toward correlation between *ACE2* expression and indirect or endogenous airway hyperresponsiveness as determined by the severity of EIB, defined by the area under the forced expiratory volume in 1 second (FEV_1) versus 30 minutes postexercise challenge time curve (*B*). (*D*) *TMPRSS2* expression correlated with baseline FEV_1. Linear regression lines are shown with the 95% confidence intervals as dotted lines. AUC30 = 30 minutes postexercise challenge time curve; TMPRSS2 = transmembrane serine protease 2.

the S protein subunits, termed "S protein priming," which is necessary for membrane fusion (1). *ACE2* and *TMPRSS2* are expressed in ciliated epithelial cells of the upper and lower airway where the initial transmission of the virus likely occurs and are expressed at high concentrations on pneumocytes in the distal lung (2). Although the upregulation of this system serves as a potential mechanism to facilitate viral entry and thus transmission, there is also evidence that upregulation of ACE2 may decrease the severity of the disease (3, 4). Thus, we questioned whether asthma, which is the most prevalent chronic medical condition in children and young adults, or respiratory viral infection, which serves as a common trigger for asthma in this population, alters the expression of either *ACE2* or *TMPRSS2*. Infections with major serotype rhinovirus, including human rhinovirus-A16 (HRV-A16) are responsible for the majority of HRV infections in children and young adults. For other respiratory viruses, it has been established that heterologous viral infection can alter the susceptibility and immune response to a second respiratory viral insult (5).

We initially examined the expression of the *ACE2* and *TMPRSS2* genes in epithelial brushings from a previously described cohort of individuals with and without asthma who were extensively characterized for airway hyperresponsiveness (AHR) and were not using controller therapy (6). We did not see any evidence of differential expression between subjects with asthma and healthy control subjects (Figures 1A and 1C), which is consistent with other emerging data (7). We did not detect any correlation between *ACE2* expression and baseline lung function or direct AHR (data not shown). However, subjects with asthma defined by both a positive methacholine challenge (i.e., direct AHR) and indirect or endogenous AHR as determined by a dry air exercise challenge to assess exercise-induced bronchoconstriction (EIB+) were found to have higher concentrations of *ACE2* expression in comparison with

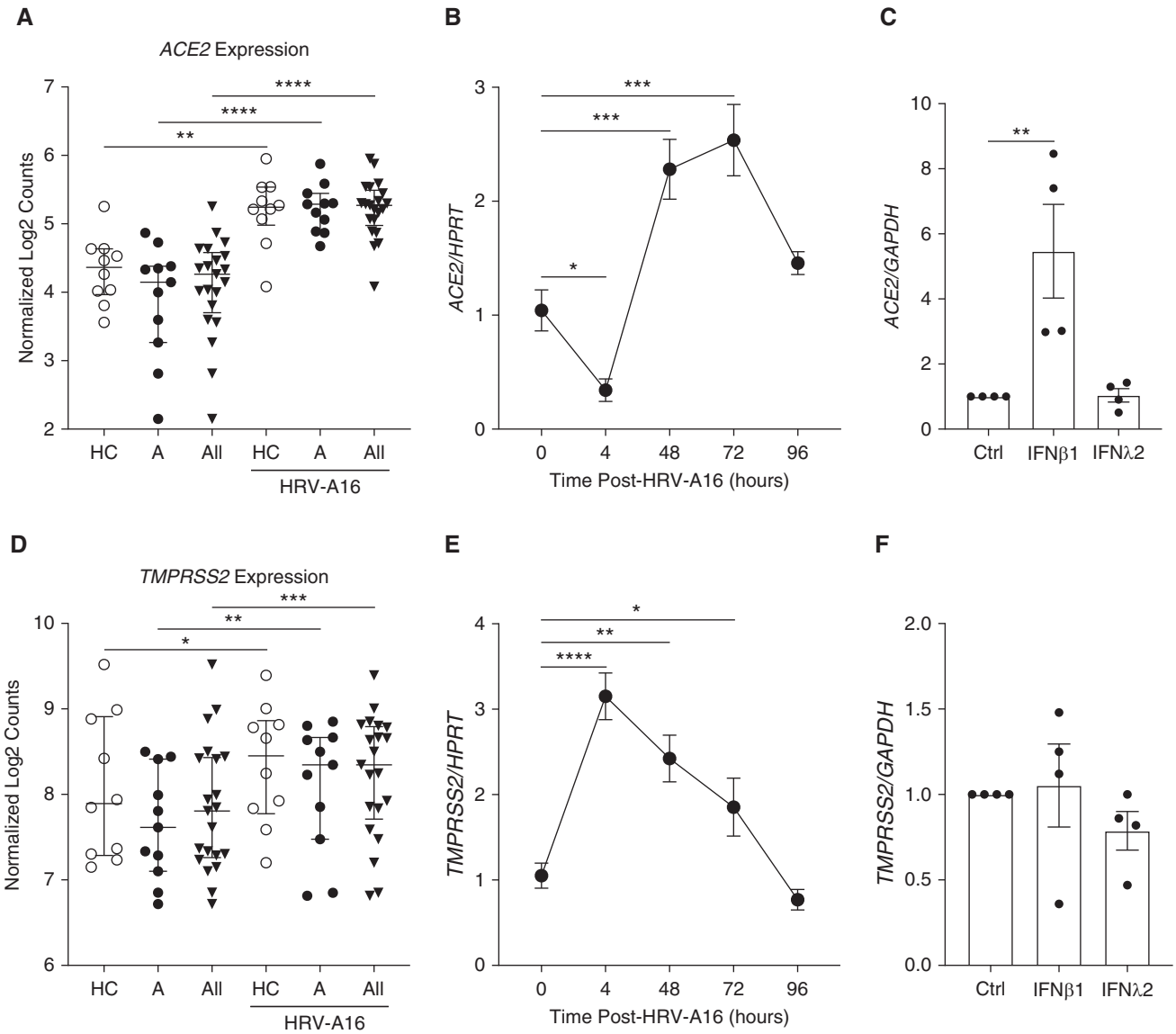

Figure 2. (*A* and *D*) RNA sequencing was performed on airway epithelial cells (AECs) obtained via blind bronchial epithelial brushings from intubated pediatric study subjects (healthy control subjects [HC], subjects with asthma [A], and all subjects [All]) and differentiated in organotypic cultures. *ACE2* expression (*A*) and *TMPRSS2* expression (*D*) were quantified by normalized log2 counts both at baseline and after infection with human rhinovirus-A16 (HRV-A16) at 48 hours. Median values with interquartile ranges are shown. *P* values comparing HC to A ± HRV-A16 represent the results of a two-way ANOVA. *P* values comparing All ± HRV-A16 represent the results of paired *t* tests. (*B* and *E*) PCR analysis was performed on nondiseased lung transplant donor AECs differentiated in air–liquid interface organotypic cultures and exposed to HRV-A16. *ACE2* (*B*) and *TMPRSS2* (*E*) expression levels in comparison with the housekeeping gene *HPRT* were assessed at various time points after infection ($n = 4$, each data point represents the mean of two PCR reactions). Mean values are shown with error bars representing the SE of the mean. *P* values represent the result of one-way ANOVA. (*C* and *F*) PCR analysis was performed on AECs from healthy control pediatric study subjects who were stimulated with IFNβ1 (1 ng/ml) and IFNλ2 (1 ng/ml) for 72 hours. *ACE2* (*C*) and *TMPRSS2* (*F*) expression levels in comparison with the housekeeping gene *GAPDH* ($n = 4$, each data point represents the mean of three PCR reactions) are shown. Mean values are shown with error bars representing the SE of the mean. The *P* value in *C* is the result of a one-way ANOVA. $^{*}P < 0.05$, $^{**}P < 0.01$, $^{***}P < 0.001$, and $^{****}P < 0.0001$. Ctrl = control; HPRT = hypoxanthine guanine phosphoribosyltransferase.

subjects with asthma without EIB (EIB−, Figure 1A). There was also a modest association between *ACE2* expression with the severity of EIB as determined by the area under the forced expiratory volume in 1 second (FEV_1) versus 30 minutes postexercise challenge time curve (AUC30) (Figure 1B). In ptcontrast, the expression of *TMPRSS2* correlated with lower baseline FEV_1 (Figure 1D) and baseline FEV_1/forced vital capacity (FVC) values ($r^2 = 0.31$; $P = 0.006$) but not direct or indirect AHR. We acknowledge the inherent limitations of this study and their impacts on our findings, particularly the small number of control subjects and the analysis of multiple subgroups.

We also examined the expression of *ACE2* and *TMPRSS2* in *ex vivo* cultured lower airway epithelial cells (AECs) from

children with and without asthma both at baseline and during infection with HRV-A16 for 48 hours (6). There were no significant differences in the age, sex, baseline FEV_1, and fraction of exhaled nitric oxide between the groups, but the children with asthma had more airflow obstruction measured by the FEV_1/FVC ratio ($P = 0.02$), significantly higher total serum IgE concentrations (mean values of 381 vs. 16 kU/L; $P = 0.01$), and higher number of positive allergen-specific IgE titers on radioallergosorbent testing (mean values, 2.7 vs. 0; $P < 0.01$) relative to healthy control children. We did not identify any difference in the baseline expression amount of *ACE2* and *TMPRSS2* between AECs cultured from children with asthma compared with healthy control children; however, there was upregulation of both *ACE2* and *TMPRSS2* expression in response to infection with HRV-A16 in AECs from children with asthma and healthy control children (Figures 2A and 2D). We further confirmed these results using primary tracheal AECs from nondiseased donors to demonstrate increased expression of *ACE2* (Figure 2B) and *TMPRSS2* (Figure 2E) after infection with HRV-A16. Interestingly, the expression pattern of these genes differs after HRV-A16 infection, as *TMPRSS2* expression increased at 4 hours postinfection and remained elevated at 72 hours (Figure 2E), whereas *ACE2* expression was decreased at 4 hours but then increased at 48 and 72 hours after infection (Figure 2B). This suggests that changes in *ACE2* and *TMPRSS2* expression after HRV infection are regulated by different mechanisms. Rhinovirus infection is known to induce a type 1 and type III IFN response in airway epithelium (8), which prompted us to stimulate pediatric AECs with IFNβ1 and IFNλ2 and evaluate their effects on *ACE2* and *TMPRSS2* expression. We found IFNβ1 stimulation resulted in increased *ACE2* expression, but IFNλ2 stimulation did not induce the expression of *ACE2* (Figure 2C). There was no effect of either IFN on *TMPRSS2* expression (Figure 2F).

Our findings demonstrate that HRV-A16 infection significantly upregulates the expression of the *ACE2* and *TMPRSS2* in epithelial cells and indicates *ACE2* expression is regulated by IFNβ1. Major serotype rhinoviruses are among the most common respiratory viral infections in children and young adults (9, 10), and upregulation of ACE2 and TMPRSS2 on AECs with symptomatic infection or asymptomatic harboring of rhinovirus could impact transmission of SARS-CoV-2 through our communities. Studies of the original SARS coronavirus suggested that the virus itself decreased *ACE2* expression and that the upregulation of ACE2 may be protective for severe disease in mice (3, 4). We expand on recently published studies that have demonstrated *ACE2* is an IFN-stimulated gene (11–13) by specifically exploring the roles of IFNβ1 and IFNλ2, which are known to be induced in the airway epithelium in response to rhinovirus infection and evaluated effects on both *ACE2* and *TMPRSS2*. These results suggest that infection with major serotype HRVs could facilitate SARS-CoV-2 transmission and modulate disease severity through IFNβ1.

Our results further refine the relationship between asthma and the expression of the *ACE2* and *TMPRSS2* in the airway epithelium by identifying relationships to AHR and lung function. Prior studies have found that individuals with asthma may have heightened susceptibility to HRV infection, and although *ex vivo* infection with HRV-A16 upregulated *ACE2* and *TMPRSS2* expression, there was no specific effect of asthma status. Our findings are concordant with initial reports suggesting that asthma is not a major risk factor for severe disease (14), but little is known about how these factors affect transmission. Our results should spur additional studies that focus on risk factors involved in SARS-CoV-2 transmission, including the prevalence of asthma and the frequency of infection or coinfection with HRVs, particularly the timing of these factors in relation to community surges of coronavirus disease (COVID-19). ■

Author disclosures are available with the text of this letter at www.atsjournals.org.

Ryan C. Murphy, M.D.
Ying Lai, Ph.D.
University of Washington
Seattle, Washington

Kaitlyn A. Barrow, B.A.
Seattle Children's Research Institute
Seattle, Washington

Jessica A. Hamerman, Ph.D.
Adam Lacy-Hulbert, Ph.D.
Benaroya Research Institute
Seattle, Washington

Adrian M. Piliponsky, Ph.D.
Seattle Children's Research Institute
Seattle, Washington

Steven F. Ziegler, Ph.D.
Benaroya Research Institute
Seattle, Washington

William A. Altemeier, M.D.
University of Washington
Seattle, Washington

Jason S. Debley, M.D., M.P.H.
Seattle Children's Hospital
Seattle, Washington
and
Seattle Children's Research Institute
Seattle, Washington

Sina A. Gharib, M.D.
Teal S. Hallstrand, M.D., M.P.H.*
University of Washington
Seattle, Washington

ORCID IDs: 0000-0003-0094-0003 (R.C.M.); 0000-0002-2480-4367 (S.A.G.).

*Corresponding author (e-mail: tealh@uw.edu).

References

1. Hoffmann M, Kleine-Weber H, Schroeder S, Krüger N, Herrler T, Erichsen S, *et al*. SARS-CoV-2 cell entry depends on ACE2 and TMPRSS2 and is blocked by a clinically proven protease inhibitor. *Cell* 2020;181:271–280, e8.
2. Sungnak W, Huang N, Bécavin C, Berg M, Queen R, Litvinukova M, *et al*.; HCA Lung Biological Network. SARS-CoV-2 entry factors are highly expressed in nasal epithelial cells together with innate immune genes. *Nat Med* 2020;26:681–687.
3. Kuba K, Imai Y, Rao S, Gao H, Guo F, Guan B, *et al*. A crucial role of angiotensin converting enzyme 2 (ACE2) in SARS coronavirus-induced lung injury. *Nat Med* 2005;11:875–879.

4. Imai Y, Kuba K, Rao S, Huan Y, Guo F, Guan B, *et al*. Angiotensin-converting enzyme 2 protects from severe acute lung failure. *Nature* 2005;436:112–116.
5. Chen HD, Fraire AE, Joris I, Welsh RM, Selin LK. Specific history of heterologous virus infections determines anti-viral immunity and immunopathology in the lung. *Am J Pathol* 2003;163:1341–1355.
6. Altman MC, Lai Y, Nolin JD, Long S, Chen CC, Piliponsky AM, *et al*. Airway epithelium-shifted mast cell infiltration regulates asthmatic inflammation via IL-33 signaling. *J Clin Invest* 2019;129: 4979–4991.
7. Peters MC, Sajuthi S, Deford P, Christenson S, Rios CL, Montgomery MT, *et al*. COVID-19-related genes in sputum cells in asthma: relationship to demographic features and corticosteroids. *Am J Respir Crit Care Med* 2020;202:83–90.
8. Khaitov MR, Laza-Stanca V, Edwards MR, Walton RP, Rohde G, Contoli M, *et al*. Respiratory virus induction of alpha-, beta- and lambda-interferons in bronchial epithelial cells and peripheral blood mononuclear cells. *Allergy* 2009;64:375–386.
9. Mäkelä MJ, Puhakka T, Ruuskanen O, Leinonen M, Saikku P, Kimpimäki M, *et al*. Viruses and bacteria in the etiology of the common cold. *J Clin Microbiol* 1998;36:539–542.
10. Tregoning JS, Schwarze J. Respiratory viral infections in infants: causes, clinical symptoms, virology, and immunology. *Clin Microbiol Rev* 2010;23:74–98.
11. Ziegler CGK, Allon SJ, Nyquist SK, Mbano IM, Miao VN, Tzouanas CN, *et al*.; HCA Lung Biological Network. Electronic address:lung-network@humancellatlas.org; HCA Lung Biological Network. SARS-CoV-2 receptor ACE2 is an interferon-stimulated gene in human airway epithelial cells and is detected in specific cell subsets across tissues. *Cell* 2020;181:1016–1035, e19.
12. Chua RL, Lukassen S, Trump S, Hennig BP, Wendisch D, Pott F, *et al*. COVID-19 severity correlates with airway epithelium-immune cell interactions identified by single-cell analysis. *Nat Biotechnol* 2020; 38:970–979.
13. Sajuthi SP, DeFord P, Jackson ND, Montgomery MT, Everman JL, Rios CL, *et al*. Type 2 and interferon inflammation strongly regulate SARS-CoV-2 related gene expression in the airway epithelium. *bioRxiv*; 2020 [accessed 2020 Apr 10]. Available from: https://www.biorxiv.org/content/10.1101/2020.04.09.034454v1
14. Wu Z, McGoogan JM. Characteristics of and important lessons from the coronavirus disease 2019 (COVID-19) outbreak in China: summary of a report of 72 314 cases from the Chinese center for disease control and prevention. *JAMA* 2020;323:1239–1242.

Bystander Macrophage Metabolic Shift after *Mycobacterium tuberculosis* Infection

To the Editor:

Mitochondrial metabolic changes in response to a pathogenic stimulus results in the upregulation of aerobic glycolysis in a manner similar to the Warburg effect to sustain the bioenergetic demand of an immune response. This metabolic shift ultimately determines immune cell effector polarization and has been adopted as a core paradigm in the field of immunometabolism.

In the context of pathogen-induced metabolic derangements, such as those observed during *Mycobacterium tuberculosis* infection (1, 2), it is now evident that the successful host response to *M. tuberculosis* by the macrophage induces glycolysis, which drives a proinflammatory phenotype. The microenvironment in which these infected macrophages reside also contain the rather understudied bystander immune cells. These include resident T cells and macrophages, which *in vivo*, occupy a significant proportion of the lung microenvironment. The question arises as to whether these bystander cells metabolically respond to the neighboring *M. tuberculosis* infection and whether this influences the immunobiology of the affected tissue. Besides inflammatory mediators such as cytokines and chemokines, evidence suggests that some metabolic intermediates secreted by the glycolytic cell have functions beyond self-regulation, which include sensing of microenvironmental conditions that influence the outcome of an immune response (3). This work as well as previous work by our group show that *M. tuberculosis*–infected macrophages induce dose-dependent T-cell apoptosis (4) and bystander macrophage (by-mac) apoptosis (5) and suggest that *M. tuberculosis*–infected macrophages significantly influence their bystander counterparts. Using an *in vitro* approach, we aimed to assess the metabolic responsiveness of the by-mac during an infectious episode and address whether this effect includes metabolic reprogramming of these immune cells.

We used human monocyte–derived macrophages prepared from buffy coats from healthy donors and infected them with either irradiated H37Rv (iH37Rv) or H37Ra mycobacteria at a multiplicity of infection (MOI) of 1–5 bacilli/cell as previously described (6). After a 24-hour infection period, supernatants were removed and then sterile filtered. By-macs (M0 phenotype confirmed through CD14 and CD68 expression) were then exposed to either the H37Ra or iH37Rv supernatant for 90 minutes prior to either confocal microscopy or metabolic measurements, as it has been established that glycolytic induction occurs within 120 minutes of stimulus exposure (7). Mitochondrial morphological assessment was accomplished by staining with MitoTracker Red CMXRos and staining iH37Rv bacteria with PKH67 membrane dye (green) on the morning of infection. Metabolic measurements using the Mito Stress test were assessed using the Seahorse XF extracellular flux analyzer (*see* online supplement).

Because changes in mitochondrial morphology are associated with metabolic changes within the cell (8), we first sought to determine whether supernatants from iH37Rv- and H37Ra-infected cells induced changes in mitochondrial morphology from by-macs (Figure 1A). Using macrophages infected with iH37Rv (green) for 24 hours as a comparison, confocal microscopic examination revealed increased mitochondrial fragmentation in by-macs, as evidenced by an increase in small, punctate mitochondria in both supernatant-treated groups. To determine whether this morphological change accompanied changes in the bioenergetics of the cell, we utilized the Seahorse XF Flux analyzer and the Mito Stress test (Figures 1B–1E). Current metabolic profiles examined during *M. tuberculosis* infection provide collective data for a mixed population of macrophages (i.e., both infected and by-macs are simultaneously assessed), which is an aspect we address in this study. We observed that by-macs exposed to supernatants had significantly lower basal oxygen consumption rates (OCRs) in comparison to the control group. Furthermore, maximal OCR in all three experimental groups was significantly reduced (Figure 1C). Additionally, we noted that basal extracellular acidification rate (ECAR) was significantly

Supported by the Royal City of Dublin Hospital Trust.

This letter has a data supplement, which is accessible from this issue's table of contents at www.atsjournals.org.